17th World Conference on Earthquake Engineering, 17WCEE
Sendai, Japan - September 13th to 18th 2020

CASE STUDY ON SEISMIC HEBAVIOR OF AN INNOVATIVE STRUCTURAL SYSTEM FOR PREFABRICATED CONSTRUCTION

He Zhao[(1)], Mu-Xuan Tao[(2)]*, Xin Nie[(3)], Zhao-Xin Hou[(4)], Chao Gong[(5)], Chen Wang[(6)]

[(1)] *PhD candidate, Tsinghua University (China), zhaohe0626@163.com*
[(2)] *Associate Professor, Tsinghua University (China), taomuxuan@mail.tsinghua.edu.cn*
[(3)] *Associate Professor, Tsinghua University (China), xinnie@tsinghua.edu.cn*
[(4)] *Engineer, Central Research Institute of Building and Construction, MCC Group, Co., Ltd (China), hzxlxl@sina.com*
[(5)] *Engineer, Central Research Institute of Building and Construction, MCC Group, Co., Ltd (China), gongchao6330@163.com*
[(6)] *PhD candidate, Tsinghua University (China), qtwjy309@163.com*

Abstract

Nowadays, prefabricated structures have drawn more and more attention due to quick construction and low cost. Based on the developing demand of prefabricated construction, an innovative composite structural system with separated gravity and lateral resisting systems is proposed in this paper. The structural scheme of this new system is designed for an office building and comparative study is conducted on the seismic behavior of the new structural system with traditional rigid composite structural system. In the basis of the design results of the two structural systems, nonlinear time history analyses with the self-developed three-dimensional finite element program COMPONA-FIBER are carried out. The self-vibration properties, dynamic responses, force mechanisms and structure failure modes under earthquake action are discussed in detail. The analysis results indicate that the new structural system demonstrates totally different deformation patterns, mechanical characteristics and failure modes from the traditional system. The deformation patterns of the new structural system are mainly composed of flexural deformation and the inter-story drift ratio of the top story is the maximum. The force at the bottom of the shear walls and columns in the new structural system is the highest acting as a cantilever, and the shear walls bear most of the earthquake action. All the beams in the new structural system are simply supported only bearing gravity loads, which are suitable for standardized design and fabrication. The damage of the new structural system under severe earthquake concentrates in the shear walls, which are the most severely damaged at the bottom.

Keywords: innovative structural system; seismic behavior; prefabricated construction; nonlinear time history analysis

1. Introduction

Prefabricated structures have advantages of fast construction, low cost and environmental protection compared to traditional cast-in-place structures. Therefore, prefabricated structures have been widely applied in projects since the 20th century [1]. Different structural systems which are suitable for prefabricated construction are proposed and investigated through experimental and finite element calculating methods [2–6]. However, most of these prefabricated structures are only applied in areas with low seismic fortification requirements and contain no more than three stories due to the insufficient earthquake resistance capacity. Considering the deficiencies of previous research, an innovative composite structural system with separated gravity and lateral resisting systems (SGLR system for short) is proposed for the application of prefabricated construction in areas with high seismic fortification intensity in this paper. The sketch of the SGLR system and traditional composite structural system (traditional system for short) is shown in Fig. 1. All beams in the SGLR system are simply supported to achieve standardized production, and shear walls are used as the main lateral resistant components. In order to evaluate the seismic behavior of the SGLR system, a comparison between the responses of the SGLR system and traditional system under earthquake action is conducted based on a real project using self-developed three-dimensional finite element program COMPONA-FIBER [7].

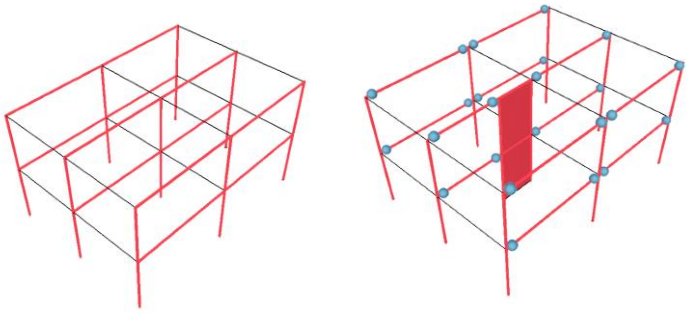

(a) Traditional system (b) SGLR system

Fig. 1 – Sketch of the traditional system and SGLR system

2. Structural design of the two structural systems

2.1 Overview of the investigated structure

The investigated structure is a six-story office building located in Beijing, China. The structural layout of the building is shown in Fig. 2. The structural design of the building followed *Chinese Code for design of composite structures* [8] and *Chinese Code for seismic design of buildings* [9]. The characteristic dead load and live load for the building are 6.0 kN/m^2 (including the weight of slabs and walls) and 3.0 kN/m^2, respectively. The design maximum spectrum value α_{max} equals 0.16 for frequent earthquake level and 0.90 for severe earthquake level [10]. The characteristic period T_g of design spectrum is 0.45s.

2.2 Structural design of traditional system

Concrete-filled rectangular steel tubular columns (CFRSTC) and I-shaped steel-concrete composite beams are adopted in the traditional system. The strength grade of steel is Q345 (with standard yield strength of 345 MPa). C40 concrete (with design compressive strength of 19.1 MPa) and C40 concrete (with design compressive strength of 14.3 MPa) are used for CFRSTC columns and slabs, respectively. The information of the key components is summarized in Table 1. Double-decked reinforcements with the spacing of 150 mm and diameter of 10 mm were cast in the 120mm-thick concrete slabs.

© The 17th World Conference on Earthquake Engineering

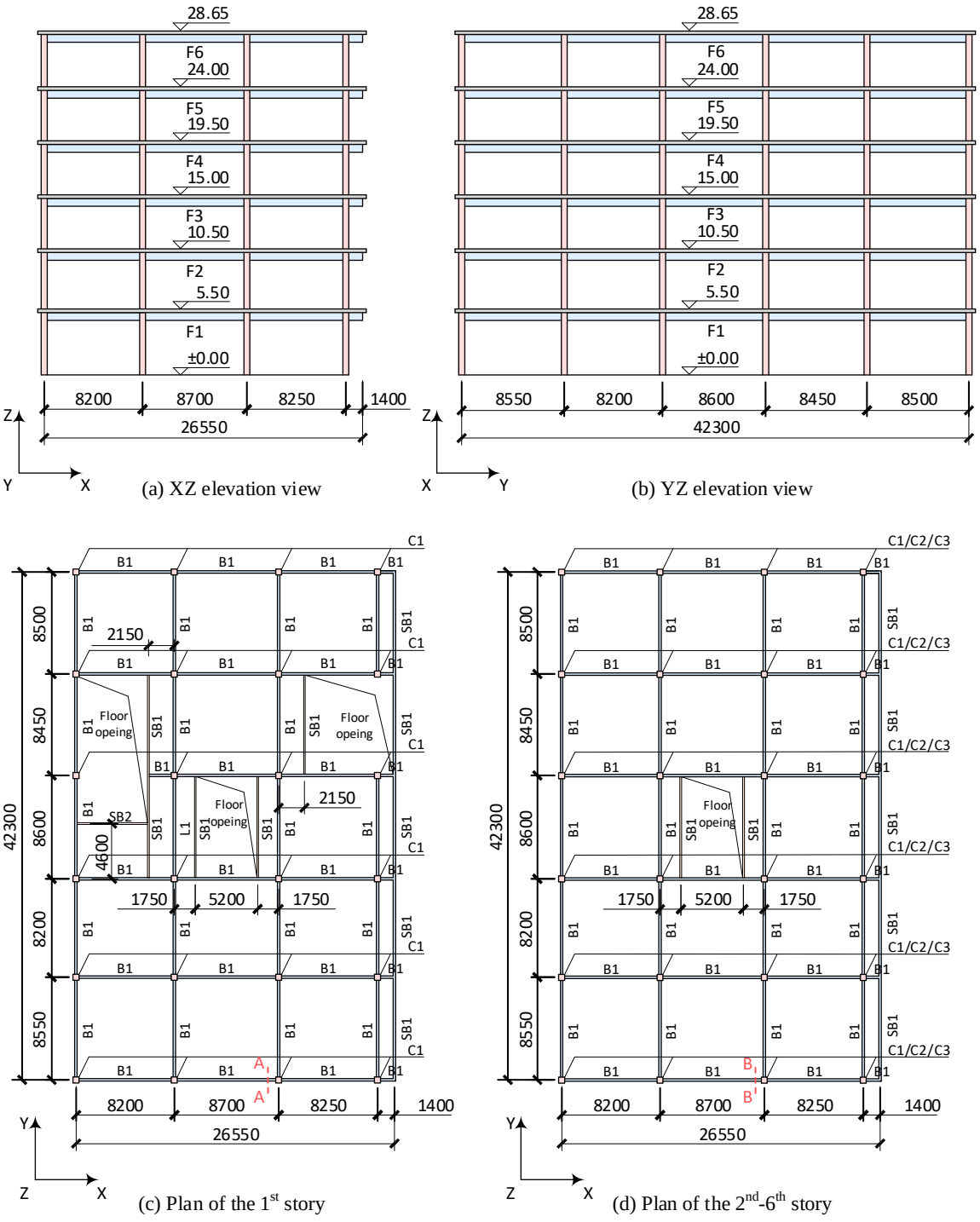

Fig. 2 – Structural layout of the investigated building

Table 1 – Information of key components in traditional system

Component number	Usage	Component type	Cross section size (mm)			
			$b(h_s)$	$h(b_f)$	t_w	t_f

© The 17th World Conference on Earthquake Engineering

C1	Columns of 1st-2nd story	CFRSTC columns	550	550	18	18
C2	Columns of 3rd-4th story	CFRSTC columns	500	500	18	18
C3	Columns of 5th-6th story	CFRSTC columns	500	500	16	16
B1	Primary beams	I-shaped composite beams	500	250	16	22
SB1	Secondary beams	I-shaped composite beams	500	250	16	22
SB2	Secondary beams	I-shaped composite beams	200	150	8	12

Note: b and h are the width and height of the section of CFRSTC columns, respectively; h_s and b_f are the height and flange width of the steel beams, respectively; t_w and t_f are the thickness of the webs and flanges of the steel beams, respectively.

2.3 Structural design of the SGLR system

The structural layout of the SGLR system is shown in Fig. 3. In order to increase the lateral resistance of the structure in both directions, four pieces of concrete filled composite plate shear walls (CPSW) numbered as W1 are arranged at the four corners of the structure along the X direction, and two pieces of CPSW walls numbered as W2 are arranged in the center of the structure along the Y direction. In addition, the arrangement of shear walls at the corners of the structure can improve the torsional resistance, thereby remedying the problem of insufficient torsional stiffness of the overall structure caused by the hinged connections.

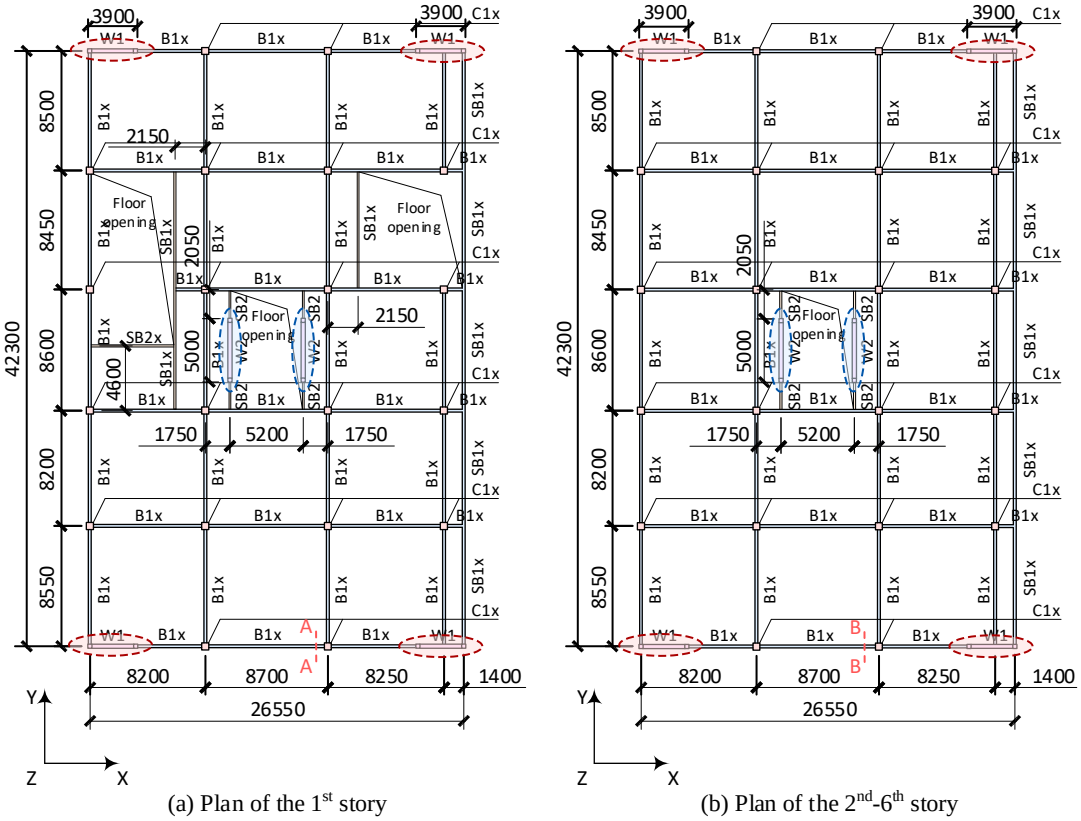

(a) Plan of the 1st story

(b) Plan of the 2nd-6th story

Fig. 3 – Structural layout of SGLR system

© The 17th World Conference on Earthquake Engineering

Since there are no current codes for the design of the SGLR system, the beams and columns are still designed according to the requirements applicable to the traditional system, and the dimensions of CPSW walls are determined by the criterion that the maximum inter-story drift ratio of the SGLR system is equal to that of the traditional system. Considering that the maximum inter-story drift ratio is a key indicator for measuring the seismic resistance of structures during the elastic design stage, the design criterion can ensure that the two structural systems are comparable to a certain extent. The design results of the key components for the SGLR system are given in Table 2.

Table 2 – Information of key components in the SGLR system

Component number	**Usage**	**Component type**	**Cross section size (mm)**			
			$b(h_s)$	$h(b_f)$	t_w	t_f
C1x	Columns of 1st-6th story	CFRSTC columns	550	550	18	18
B1x	Primary beams	I-shaped composite beams	500	250	16	22
SB1x	Secondary beams	I-shaped composite beams	500	250	16	22
SB2	Secondary beams	I-shaped composite beams	200	150	8	12
W1	Walls in X direction	CPSW walls	3900×300×14			
W2	Walls in Y direction	CPSW walls	5000×300×14			

Note: The meaning of parameters of cross section size for columns and beams in the SGLR system is the same as Table 1, and the three parameters for the cross section size of CPSW walls represent the width of the wall, the thickness of the wall and the thickness of the steel plates in the walls, respectively.

3. Numerical modelling

3.1 Element and material models

The columns and beams in the two structures are modeled with self-developed fiber beam-column elements [7], which use a displacement-based distributed plasticity approach. The multi-layer shell element proposed by Lu et al. [11] is implemented to model the behavior of CPSW walls.

The uniaxial constitutive relationship of concrete and steel used in the fiber beam-column elements is shown in Fig. 4. The hysteresis rule of concrete can consider the strength degradation behavior under repeated loading and unloading. The model of steel and reinforcements can reasonably consider the Bauschinger effect under cyclic loads. In multi-layer shell elements, the concrete material adopts the elastoplastic constitutive model with von Mises yield surface and isotropic hardening rule, and the steel material adopts the elastoplastic constitutive model with von Mises yield surface and kinematic hardening rule. The main parameters in material constitutive models are given in Table 3.

3.2 Modelling methods

Finite element models of the two structures are built by MSC.MARC. Rigid floor assumption is achieved by coupling the floor nodes in X and Y directions through the RBE2 links. The vertical load on the floor and the equivalent mass considered in the seismic calculation can be realized through the RBE3 links. The representative value of gravity load, which equals the sum of dead load and half live load, is applied at the reference nodes of the RBE3 links. The floor mass is defined by the initial condition module in the software, and the specific value is determined according to the representative value of gravity load value for the floor panel. In addition, RBE2 links are adopted to simulate the hinged connections in the SGLR system.

© The 17th World Conference on Earthquake Engineering

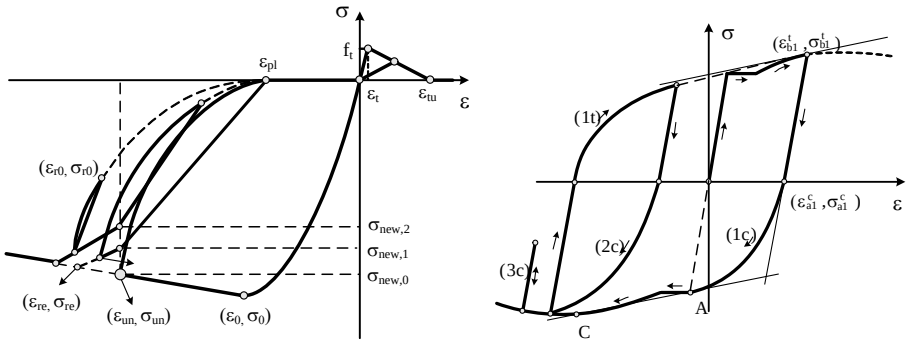

(a) Concrete (b) Steel

Fig. 4 – Uniaxial material constitutive laws in the fiber beam-column element

Table 3 – Main parameters in material constitutive models

Material	**Peak compressive stress σ_0 (Mpa)**	**Peak compressive strain ε_0**	**Tensile strength f_t (MPa)**	**Elastic modulus E (GPa)**	**Yield strength f_y (MPa)**
Concrete (C40)	32.0	0.002	3.04	32.5	-
Steel (Q345)	-	-	-	206	345
Reinforcement (HRB400)	-	-	-	206	400

4. Dynamic characteristics

The natural vibration characteristics of the two structures are evaluated first before the nonlinear time history analyses. The first nine natural vibration periods and the corresponding features of the vibration modes are given in Table 4. Due to the regular structural arrangement, there are no local modes in the first nine vibration modes of the two structures. Despite that the maximum inter-story drift ratios are controlled the same during the design stage, the natural vibration periods of the SGLR system are lower than the corresponding periods of the traditional system. It can be concluded that the arrangement of shear walls helps to increase the overall stiffness of the structure, which may not be reflected in the index of maximum inter-story drift ratios directly but can shorten the natural vibration periods.

Table 4 – Natural vibration characteristics of the two structures

Mode	Traditional system		SGLR system	
	Period (s)	Features	Period (s)	Features
1	1.481	Translation in X direction	1.403	Translation in X direction
2	1.423	Translation in Y direction	1.372	Translation in Y direction
3	1.213	Rotation around Z axis	0.949	Rotation around Z axis
4	0.464	Translation in X direction	0.238	Translation in Y direction
5	0.448	Translation in Y direction	0.234	Translation in X direction

© The 17th World Conference on Earthquake Engineering

6	0.382	Rotation around Z axis	0.161	Rotation around Z axis
7	0.251	Translation in X direction	0.094	Translation in Y direction
8	0.245	Translation in Y direction	0.089	Translation in X direction
9	0.208	Rotation around Z axis	0.062	Rotation around Z axis

The first three vibration modes of the two structural systems are shown in Fig. 5. The deformation patterns of the vibration modes for the two structures are different. The traditional system mainly demonstrates shear deformation mode, while the SGLR system mainly demonstrates flexural deformation mode.

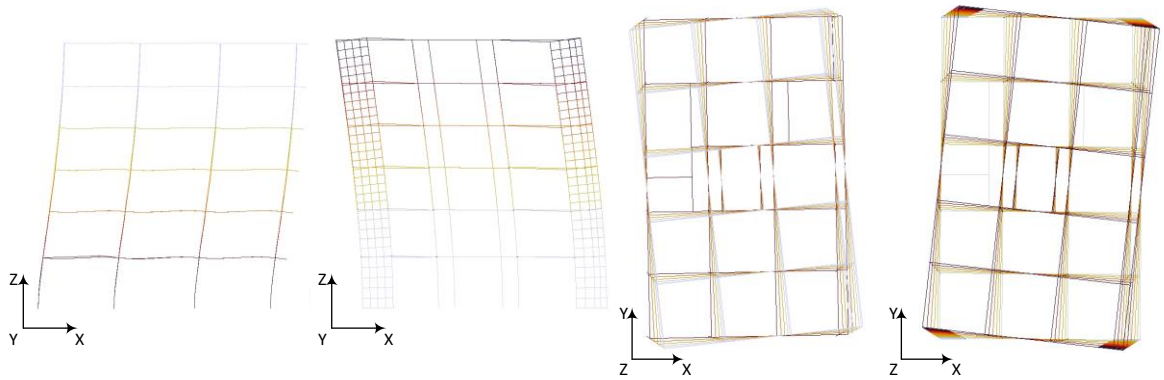

(a) Mode 1 (c) Mode 3

(b) Mode 2

Fig. 5 – First three vibration modes of the two structures

The comparison of the natural vibration characteristics of the two structures indicates that the natural vibration periods and deformation patterns of the SGLR system are different from those of the traditional system. Therefore, it is necessary to conduct further nonlinear time history analyses to study the seismic behavior of the SGLR system.

5. Nonlinear time history analyses

5.1 Ground motions

Three ground motions including two recorded accelerograms and one artificial accelerogram are chosen as inputs in the nonlinear time history analyses. The two recorded accelerograms are gained at the San Fernando station in the USA in 1971 and the Kobe station in Japan in 1995, respectively. The artificial accelerogram is generated to match the elastic response spectra stipulated by *Chinese Code for seismic design of buildings* [9].

© The 17th World Conference on Earthquake Engineering

In order to investigate the seismic performance of the two structural systems, the nonlinear time history analyses are conducted on the two structures under the action of frequent and severe earthquakes, respectively. The peak ground accelerations (PGAs) for frequent earthquakes and severe earthquakes are 0.7 m/s^2 and 4.0 m/s^2, respectively. The ground motion input is applied in both X and Y directions of the structure at the same time. For the natural ground motions, the two recorded horizontal orthogonal components are respectively applied in X and Y directions, while for the artificial ground motion, one horizontal component is applied with the PGA ratio of 1:0.85 in the two directions. The primary input direction is chosen as X and Y respectively, and thus totally 12 cases are calculated for both structures. The damping ratio is chosen as 0.04 under frequent earthquakes and 0.05 under severe earthquakes according to *Chinese Code for seismic design of buildings* [9].

5.2 Analysis results

5.2.1 Displacement responses

The roof displacements of the two structures under severe earthquakes with primary input direction X, which is the relatively weak direction indicated by the natural vibration modes, are shown in Fig. 6. It can be seen that both structures have obvious responses to the Kobe and artificial waves compared to the San Fernando wave. There is no significant difference in the amplitude of the roof displacements between the SGLR system and the traditional system. The phase positions of the roof displacements for the two structures are consistent under the San Fernando and Kobe waves while demonstrate obvious differences under the artificial wave, indicating that both the frequency spectrum of seismic waves and mechanical characteristics have effect on the displacement responses of structures under earthquake motions.

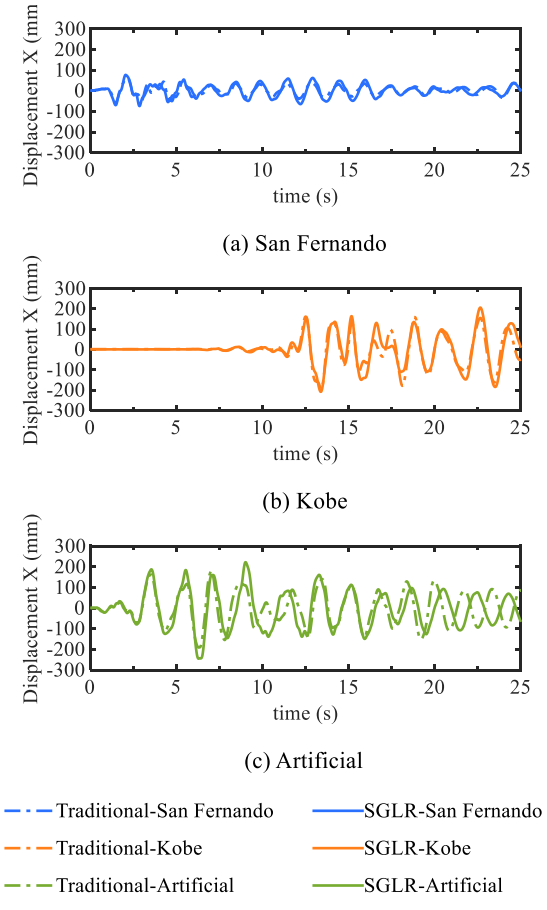

Fig. 6 – Roof displacement responses of the two structures under severe earthquakes with primary input direction X

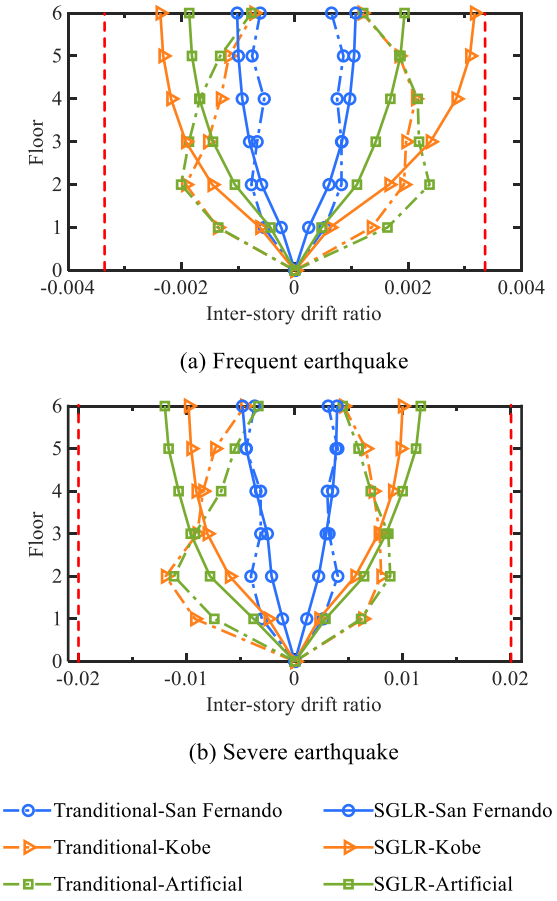

Fig. 7 – Inter-story drift ratio envelopes of the two structures under earthquakes with primary input direction X

© The 17th World Conference on Earthquake Engineering

The envelop curves of inter-story drift ratio of the two structures in X direction under frequent and severe earthquakes are plotted in Fig. 7, where the limited values stipulated by the codes [9,12] marked with red dashed lines. All the inter-story drift ratios in Fig. 7 meet the requirements, manifesting the safety of the two structures in seismic conditions. It is worth noting that the two structures demonstrate totally different deformation patterns. The floor location of the maximum inter-story drift ratio is quite different between the two structures. It can be concluded that the main deformation patterns for the traditional system and the SGLR system are shear deformation and flexural deformation, respectively, which further verifies the findings in the analysis of the vibration modes in Section 4.

In spite of the different deformation patterns between the two structures, the maximum inter-story drift ratios of the two structures in any case are quite close as shown in Table 5. In addition, the maximum inter-story drift ratios in X and Y directions are also close, indicating the uniform and reasonable arrangement of lateral resistant systems for the two structures.

Table 5 – Maximum inter-story drift ratios of the two structures

Ground motion		Traditional system		SGLR system	
		X direction	Y direction	X direction	Y direction
Frequent earthquakes	San Fernando	1/1167	1/729	1/931	1/1033
	Kobe	1/469	1/409	1/315	1/322
	Artificial	1/421	1/454	1/517	1/506
Severe earthquakes	San Fernando	1/221	1/181	1/206	1/197
	Kobe	1/84	1/92	1/100	1/100
	Artificial	1/89	1/84	1/83	1/82

5.2.2 Failure modes

The time history analyses demonstrate that both structures remain elastic under frequent earthquakes. However, under severe earthquake excitation, many plastic hinges are observed in the two structures. The development of plastic hinges for the two structures under the artificial wave, which causes the severest damage to the structures, is shown in Fig. 8. When the seismic excitation lasts 3.41s, the first batch of plastic hinges appear at the beams ends of the first and second stories for the traditional system, while the plastic hinges are also observed at the boundary column feet next to the shear walls W1 and W2 for the SGLR system. At the 6th second of the artificial wave, the number of plastic hinges in the bottom two stories increase with the appearance of plastic hinges at column feet of the first floor for the traditional system, while the plastic length of the boundary columns extends upwards for the SGLR system. When the ground motion comes to the end at the 25th second, plastic hinges develop at the beam ends of the 1st-4th stories and all the column feet of the first floor for the traditional system, while plastic hinges develop at all the boundary column feet and the plastic length of the boundary columns extends to the top of the first story, indicating that the damage of the SGLR system concentrates in the bottom of shear walls.

5.2.3 Force mechanisms

The base shear of the whole structures and internal forces of structural members of the two structures are analysed in this section to reveal the force mechanism of the SGLR system.

The time history curves of base shear of the two structures are plotted in Fig. 9. It can be seen that the shear walls bear the majority of base shear of the overall SGLR system because the lateral stiffness of shear walls is much greater than that of the columns. Additionally, the base shear of the SGLR system is usually greater

© The 17th World Conference on Earthquake Engineering

than that of the traditional system during the seismic excitation process, indicating that the arrangement of shear walls can amplify the base shear of the structure.

Figure 10 shows the time history curves of bending moments of the section A and section B in the first and fourth stories of the two structures marked in Fig. 2 and Fig. 3, respectively. It can be drawn from the comparison that the bending moments of the traditional system fluctuate greatly bearing significant positive and negative moments under the reciprocating seismic wave and the bending moment of the first story is greater than that of the fourth story. However, the bending moments at the beam ends in both the first and the fourth stories of the SGLR system are always maintained at a level close to zero without obvious change during the seismic excitation process. The differences indicate that the beams simply supported in the SGLR system only bear vertical floor loads under earthquake action, which facilitates the standard design and fabrication of beams in the SGLR system.

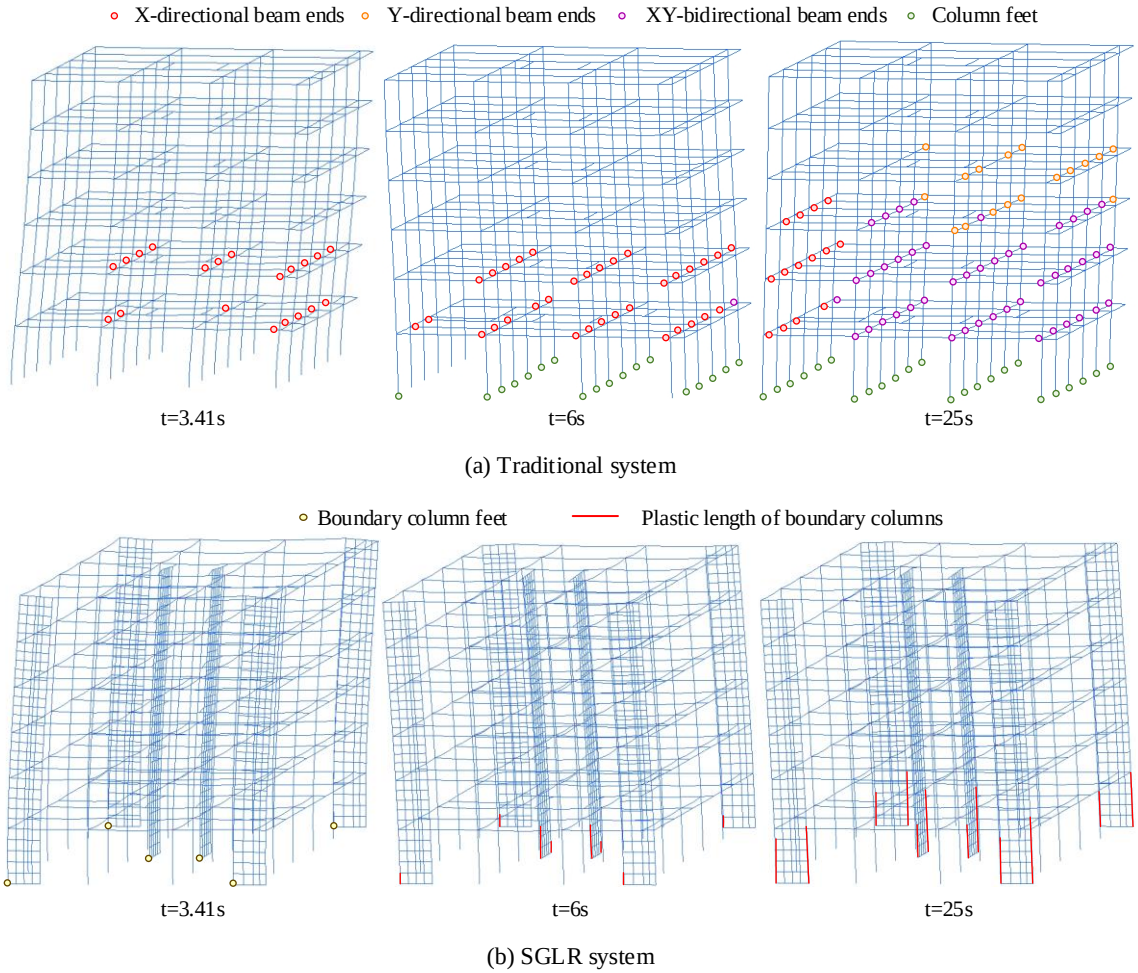

(a) Traditional system

(b) SGLR system

Fig. 8 – Distribution and development of plastic hinges of the two structures under severe earthquakes

© The 17th World Conference on Earthquake Engineering

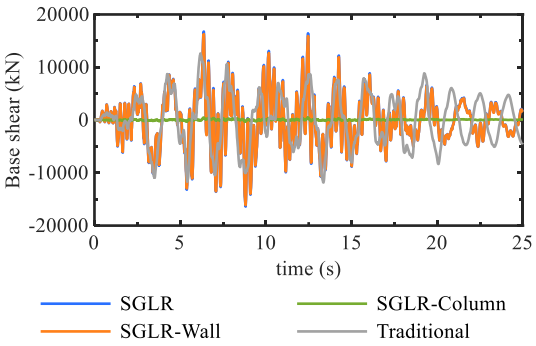

Fig. 9 –Time history curves of base shear of the two structures

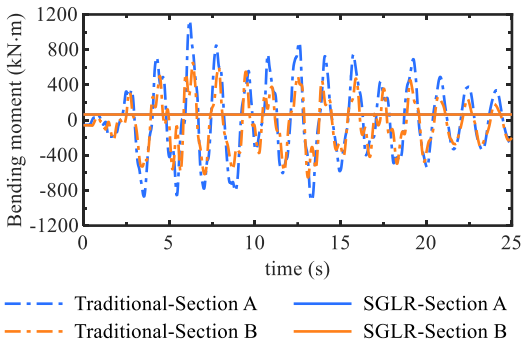

Fig. 10 –Time history curves of bending moment at beam ends of the two structures

6. Conclusions

In this paper, a case study is carried out on an innovate composite structural system with separated gravity and lateral resisting systems (SGLR system) by self-developed three-dimensional finite element program COMPONA-FIBER. The natural vibration characteristics, deformation patterns, failure modes and force mechanisms of the SGLR system are discussed in detail compared to those of the traditional system. The major conclusions are drawn as follows:

The SGLR system mainly demonstrates the flexural deformation pattern under horizontal earthquake action with the maximum inter-story drift ratio occurring at the top story.

The failure modes of the SGLR system are quite different from those of the traditional system under severe earthquakes. The damage concentrates in the bottom of shear walls and boundary columns of the SGLR system. Therefore, the shear walls in the bottom story need strengthening measures in construction.

The shear walls bear most of the base shear in the SGLR system under seismic action and can amplify the base shear of the structure compared to the traditional system.

The beams in the SGLR system can be standardized for design and fabrication due to the constant internal forces during the seismic excitation process, indicating that the SGLR system is suitable to be applied in prefabrication construction.

7. Acknowledgements

The writers gratefully acknowledge the financial support provided by the National Natural Science Foundation of China (Grant No. 51878378).

8. References

[1] Navaratnam S, Ngo T, Gunawardena T, Henderson D. Performance Review of Prefabricated Building Systems and Future Research in Australia. *Buildings*. 2019;9(2):38. doi:10.3390/buildings9020038

[2] Priestley MJN, Sritharan S (Sri), Conley JR, Stefano Pampanin S. Preliminary Results and Conclusions From the PRESSS Five-Story Precast Concrete Test Building. *PCI J*. 1999;44(6):42-67. doi:10.15554/pcij.11011999.42.67

[3] Goggins JM, Broderick BM, Elghazouli AY, Lucas AS. Experimental cyclic response of cold-formed hollow steel bracing members. *Eng Struct*. 2005;27(7):977-989. doi:10.1016/j.engstruct.2004.11.017

[4] Corte GD, Fiorino L, Landolfo R. Seismic Behavior of Sheathed Cold-Formed Structures: Numerical Study. *J Struct Eng*. 2006;132(4):558-569. doi:10.1061/(ASCE)0733-9445(2006)132:4(558)

© The 17th World Conference on Earthquake Engineering

[5] Rahman MA, Sritharan S. Performance-Based Seismic Evaluation of Two Five-Story Precast Concrete Hybrid Frame Buildings. *J Struct Eng*. 2007;133(11):1489-1500. doi:10.1061/(ASCE)0733-9445(2007)133:11(1489)

[6] Pourabdollah O, Farahbod F, Rofooei FR. The seismic performance of K-braced cold-formed steel shear panels with improved connections. *J Constr Steel Res*. 2017;135:56-68. doi:10.1016/j.jcsr.2017.04.008

[7] Tao M-X, Nie J-G. Fiber Beam-Column Model Considering Slab Spatial Composite Effect for Nonlinear Analysis of Composite Frame Systems. *J Struct Eng*. 2014;140(1):04013039. doi:10.1061/(ASCE)ST.1943-541X.0000815

[8] JGJ 138–2016. *Code for Design of Composite Structures*. Beijing, China: China Architecture & Building Press; 2016. (in Chinese).

[9] GB 20011–2010. *Code for Seismic Design of Buildings*. Beijing, China: China Architecture & Building Press; 2010. (in Chinese).

[10] Shi G, Hu F, Shi Y. Comparison of seismic design for steel moment frames in Europe, the United States, Japan and China. *J Constr Steel Res*. 2016;127:41-53. doi:https://doi.org/10.1016/j.jcsr.2016.07.009

[11] Lu X, Lu X, Guan H, Ye L. Collapse simulation of reinforced concrete high-rise building induced by extreme earthquakes. *Earthq Eng Struct Dyn*. 2013;42(5):705-723. doi:10.1002/eqe.2240

[12] GB 50936-2014. *Technical Code for Concrete Filled Steel Tubular Structures*. Beijing, China: China Architecture & Building Press; 2014. (in Chinese).

© The 17th World Conference on Earthquake Engineering